Risk Analysis, Vol. 15, No. 2, 1995

The Sizes, Shapes, and Mineralogy of Asbestos Structures that Induce Lung Tumors or Mesothelioma in AF/HAN Rats Following Inhalation[1]

D. Wayne Berman,[2] Kenny S. Crump,[3] Eric J. Chatfield,[4] John M.G. Davis,[5] and Alan D. Jones[5]

Data from inhalation studies in which AF/HAN rats were exposed to nine different types of asbestos dusts (in 13 separate experiments) are employed in a statistical analysis to determine if a measure of asbestos exposure (expressed as concentrations of structures with defined sizes, shapes and mineralogy) can be identified that satisfactorily predicts the observed lung tumor or mesothelioma incidence in the experiments. Due to limitations in the characterization of asbestos structures in the original studies, new exposure measures were developed from samples of the original dusts that were re-generated and analyzed by transmission electron microscopy using a direct transfer technique. This analysis provided detailed information on the mineralogy (i.e., chrysotile, amosite, crocidolite or tremolite), type (i.e., fiber, bundle, cluster, or matrix), size (length and width) and complexity (i.e., number of identifiable components of a cluster or matrix) of each individual structure.

No univariate measure of exposure was found to provide an adequate description of the lung tumor responses observed among the inhalation studies, although the measure most highly correlated with tumor incidence is the concentration of structures ≥20 μm in length. Multivariate measures of exposure were identified that do adequately describe the lung tumor responses. Structures contributing to lung tumor risk appear to be long (≥5 μm) thin (0.4 μm) fibers and bundles, with a possible contribution by long and very thick (≥5 μm) complex clusters and matrices. Potency appears to increase with increasing length, with structures longer than 40 μm being about 500 times more potent than structures between 5 and 40 μm in length. Structures <5 μm in length do not appear to make any contribution to lung tumor risk. This analysis did not find a difference in the potency of chrysotile and amphibole toward the induction of lung tumors. However, mineralogy appears to be important in the induction of mesothelioma with chrysotile being less potent than amphibole.

KEY WORDS: Asbestos; tumorigenicity; lung tumors; mesothelioma; inhalation; dose/response; AF/HAN rats.

INTRODUCTION

Inhalation of asbestos dust has been clearly linked to lung cancer and mesothelioma in a broad range of human exposure settings; more than 50 positive epidemiology studies have now been published.[1] However, a quantitative dose-response relationship that applies across exposure environments has not been established for either disease; potency estimates derived from dif-

[1] This research was completed under contract to the U.S. Environmental Protection Agency. Such support, however, does not signify that the contents of this paper necessarily reflect the views and policies of the U.S. Environmental Protection Agency, nor does the mention of trade or commercial products constitute endorsement or recommendation for use.

[2] ICF Kaiser Engineers, Oakland, California.
[3] ICF Kaiser Engineers, Ruston, Louisiana.
[4] Chatfield Technical Consulting Limited, Mississauga, Ontario, Canada.
[5] Institute of Occupational Medicine, Edinburgh, United Kingdom.

0272-4332/95/0400-0181$07.50/1

ferent epidemiological studies differ by up to 600-fold for lung cancer (Table 6-10 of an HEI-AR report[1]) and potency estimates reported for mesothelioma induction are also quite variable.

Although there are many features of epidemiological studies that may contribute to the variability observed in dose-response relationships, a major component may be the inadequate characterization of the asbestos dusts to which individuals are exposed in the epidemiological studies. In most epidemiological studies, asbestos dust concentrations were measured (if at all) by phase contrast microscopy (PCM) or by midget impinger.[2] The impingers produce a count of total dust particles that are frequently converted to PCM-equivalent counts when comparison data are available, although the correlations are generally poor.[2] PCM measurements may not be useful for distinguishing among exposure environments that differ in their potential to induce disease because (1) PCM is not capable of distinguishing asbestos from non-asbestos structures[3] and (2) existing animal studies suggest that asbestos structures outside the range of sizes visible by PCM may contribute to risk.[1]

Because of the limitations in the characterization of asbestos exposures in epidemiological studies, the best information regarding the effects of size and mineralogy on the relative potency of asbestos structures has come from animal studies. Injection and implantation experiments (in which asbestos or other fibrous material is either injected or implanted into the pleura or peritonea of rats) generally indicate that long, thin fibers exhibit the greatest tendency to induce mesothelioma.[4-31] However, injection and implantation experiments bypass the processes associated with inhalation, retention in the lungs, and transport from the lungs, which may be important in modulating the effects of airborne exposure. Thus, results obtained from animal inhalation studies are likely to be more relevant for evaluating human risk than injection and implantation experiments.

A number of inhalation studies have been conducted in which animals (generally rats) have been exposed to varying concentrations of asbestos dusts of various types and the incidence of tumors observed in the animals recorded.[7-13,26,28,32-36] In addition to verifying that different types of asbestos can cause lung cancer and mesothelioma when inhaled by animals, these studies generally indicate that longer fibers tend to be more carcinogenic than shorter ones. However, no measure of asbestos exposure that satisfactorily predicts tumor incidence is identified in these studies.

In this study, data on tumor incidence in AF/HAN rats from 13 inhalation experiments reported in a series of studies conducted by Davis et al.[7-13] are combined in a statistical analysis to determine if a measure of exposure can be identified that satisfactorily predicts lung tumor or mesothelioma incidence. Because of limitations in the characterization of asbestos exposures in the original Davis et al. studies (use of scanning electron microscopy precluded observation of structures thinner than 0.2 μm; only SEM visible fibers and bundles were included in the characterized size distributions while clusters and matrices may also contribute to tumorigenicity in a unique way; and lack of bivariate characterization of the size distributions precluded evaluation of the combined effects of structure length and width), archived samples of the original stock samples were used to regenerate asbestos dust clouds that were collected on filters and characterized in detail by transmission electron microscopy (TEM). TEM is capable of detecting and identifying even the thinnest asbestos structures.

DATABASE AND METHODS

The Animal Inhalation Database

The series of animal studies by Davis et al.[7-11,13] all employed a common protocol, utilized the same strain of rat, and were conducted in the same laboratory by the same group of investigators. In these studies, groups of 40 male AF/HAN rats, aged 3 months at the beginning of the experiment, were exposed by inhalation for 7 hours per day, 5 days per week for 224 days over one year and then observed for a minimum of an additional year. These studies involved UICC crocidolite, Korean tremolite, four types of chrysotile and three types of amosite (Table 1). Several of the samples were also studied at two doses or on multiple occasions. Details of the experimental procedures used in these studies (along with the sources of the asbestos samples employed) are reported in the studies cited in Table 1. Due to the small number of mesotheliomas observed, the present evaluation was limited primarily to lung tumors. Benign and malignant lung tumors were pooled for this evaluation. Also, control groups from the various studies were combined into a single group.

Regeneration and Analysis of Dusts from the Animal Studies

To obtain more definitive characterization of the asbestos dusts used in the Davis et al. studies, dusts were

Table 1. Summary Data for Animal Inhalation Experiments Conducted by Davis and Coworkers[a]

Fiber type	Description	Abbreviations	Mass concentration (mg/m³)	PCM f/ml	Number of animals	Number of benign pulmonary tumors	Number of malignant pulmonary tumors	Total number of pulmonary tumors	Mesotheliomas	Reference
Chrysotile	UICC-A	UC	2	390	42	6	2	8	1	(7)
Chrysotile	UICC-A	UC	10	1,950	40	7	8	15	0	(7)
Chrysotile	Long	LC	10	5,510	40	8	12	20	3	(13)
Chrysotile	Short	SC	10	1,170	40	1	6	7	1	(13)
Chrysotile	UICC-A	UC	9.9	2,560	36	6	8	14	0	(12)
Chrysotile	UICC-A (Discharged)[b]	DC	9.9	2,670	39	4	6	10	1	(12)
Chrysotile	WDC Yarn[c]	WC	3.6	679	41	5	13	18	0	(11)
Amosite	UICC	UA	10	550	43	2	0	2	0	(7)
Amosite	Long	LA	10	2,060	40	3	8	11	3	(10)
Amosite	Short	SA	10	70	42	0	0	0	1	(10)
Crocidolite	UICC	UR	4.9	430	43	2	0	2	1	(7)
Crocidolite	UICC	UR	10	860	40	1	0	1	0	(7)
Tremolite	Korean	KT	10	1,600	39	2	16	18	2	(9)
None	Control	C	0		20	0	0	0	0	(7)
None	Control	C	0		36	0	0	0	0	(9)
None	Control	C	0		61	1	1	2	0	(10)
None	Control	C	0		64	1	1	2	0	(11)
None	Control	C	0		47	1	1	2	0	(13)

[a] Exposure occurred for 7 hours a day, 5 days a week for 1 year.
[b] UICC-A Chrysotile in this experiment was treated with mixed polarity air (produced with a source of beta radiation) following generation to reduce the surface charge on individual particles within the dust.
[c] Chrysotile samples used for dust generation in this experiment were obtained from material treated by a commercial wet dispersion process.

regenerated from samples archived from the original studies using the same equipment, procedures, and personnel as in the original studies. For each asbestos sample type, three or four sets of filters at three different particle loadings were collected at regular time intervals over approximately one hour during which the rate of dust generation was kept constant. The set of optimally-loaded filters (one from each time interval) was then prepared and analyzed and the results from the individual filters were combined. A separate set of filters was also collected for PCM analysis at the same time as the filters collected for analysis by TEM. A detailed discussion of the preparation and analysis of samples for this study and a characterization of the samples based on this analysis is currently in preparation (Berman et al., Journal article in preparation).

The regenerated dusts were analyzed by TEM using the counting criteria from the Interim Superfund Method for the Determination of Asbestos in Air.[37] These criteria provide that, in addition to examination of a portion of each filter in which all asbestos structures present are identified, a separate examination of a different portion of each filter is performed at lower magnification, during which only structures ≥ 5 μm in length are evaluated. The stopping rules in the Superfund method were modified for this study to assure that a minimum of 200 structures derived from total structure examination and, separately, 200 structures derived from examination for long structures (≥ 5 μm in length) would be evaluated for each sample. By using a separate examination for long structures, the present study achieves a level of precision for the determination of long structures that could otherwise require the counting of thousands of structures when all sizes are evaluated simultaneously.[38]

In the data base developed from the regenerated dusts, fibers, bundles, clusters and matrices (as defined in the literature[4,37]) are characterized separately along with measurements of the length and width of each such structure. Up to five fibers and bundles that are components of clusters or matrices are also characterized for those complex structures (i.e., clusters and matrices) where individual fibers or bundles can be characterized.[38] In the analyses reported herein, two methods of utilizing information on complex structures are applied. In one set of analyses, only the primary structures enter the analysis. In a second set of analyses, whenever com-

ponent fibers or bundles in a cluster or matrix are characterized; these components are included as if they are independent structures and the parent cluster or matrix is not included.

Estimation of Exposure Concentrations

Concentrations of asbestos structures in each regenerated dust that exhibit specific characteristics based on size or type were calculated by multiplying the number of structures in a particular sample displaying the characteristic(s) of interest by the total area of the filters exposed during air sample collection and dividing by the product of the area of the portion of the filters examined during the analysis and the volume of air passed through the filters during air sample collection. The concentrations of structures in the original dusts to which the animals were exposed were estimated by multiplying the corresponding concentration in the regenerated dust by the ratio of the concentration measured by PCM in the original dust to the PCM concentration in the regenerated dust.

Statistical Methods

Once the re-generated dusts were characterized, a statistical analysis was performed to test for relationships between the size, shape, and mineral type of an asbestos structure and its relative potency for inducing lung tumors. In the statistical methods employed, the probability of a lung tumor (benign or malignant) response in an animal is assumed to be of the form:

$$P = 1-\exp(-\alpha-\beta*WC) \qquad (1)$$

where α specifies the response probability in unexposed animals (*i.e.*, the probability of a response in unexposed animals is $1 - \exp[-\alpha]$), β represents the absolute potency of a dust for producing a tumor response, and WC is a weighted sum of the concentrations of structures in different structure categories. A structure category is defined by restrictions on structure sizes (*e.g.*, a defined range of lengths, widths, and/or aspect ratios) and structure types (*e.g.*, fibers, bundles, clusters, and/or matrices). The weights in the weighted sum are estimates of the relative potencies of structures in the different structure categories. Thus,

$$WC = q_1*x_1+q_2*x_2+\ldots+q_k*x_k = \Sigma q_j x_j \qquad (2)$$

where x_j is the concentration of airborne asbestos structures in the jth structure category and q_j represents the potency of structures in the jth structure category relative to the potency of structures in other categories.

The q_js are constrained to be non-negative ($q_j \geq 0$ for $j = 1, \ldots, k$) and to sum to one ($q_1 + \ldots + q_j = 1$). The latter constraint makes each q_j a measure of relative potency rather than absolute potency. The non-negativity constraint implies that no category of structures is capable of reducing the probability of a tumor response.

In a few of the analyses the model is expanded to permit the probability of response to depend upon the chemical composition (mineralogy) of the structures (*e.g.*, chrysotile or amphibole). This expanded version of the model is of the form:

$$P_i = 1-\exp(-\alpha-\beta_i*WC) \qquad (3)$$

where P_i is the probability of tumor response in animals exposed exclusively to material of type i, and β_i a measure of the absolute potency of this material. Thus, in this more general model, a different absolute potency is assumed for materials of differing mineralogy but the relative potencies of structures in different structure categories are assumed to be independent of mineralogy.

In still other analyses, the tumorigenic potential of a structure is assumed to be embodied in a single quantitative measure (*e.g.*, the surface area of the structure). In these analyses the probability of a tumor response in an animal is assumed to be of the form:

$$P = 1-\exp(-\alpha-\beta*SM) \qquad (4)$$

where SM is the sum of the quantitative measures over the structures contained in a specified volume of air. For example, if the quantitative measure is surface area, then SM is the total surface area of structures per milliliter of air.

The parameters of these models (α, β and q_j) are estimated using maximum likelihood methods and likelihood ratio tests are used for testing hypotheses.[39] Confidence intervals for individual parameters are constructed using the "profile likelihood method."[39] The goodness-of-fit of each model to the data is assessed by applying a chi-square distribution to the deviance statistic.[40] The p-value of the chi-square statistic is approximated using the chi-square distribution with degrees of freedom equal to the [number of dose groups] − [number of q_j's estimated as being non-zero] − 1.

The non-negativity constraints imposed on these models make this approach very different from ordinary (unconstrained) regression. In ordinary regression, a perfect fit of a model is guaranteed whenever the number of parameters equals or exceeds the number of data points. However, in the constrained model described above, typically all but a few of the q_j's are estimated

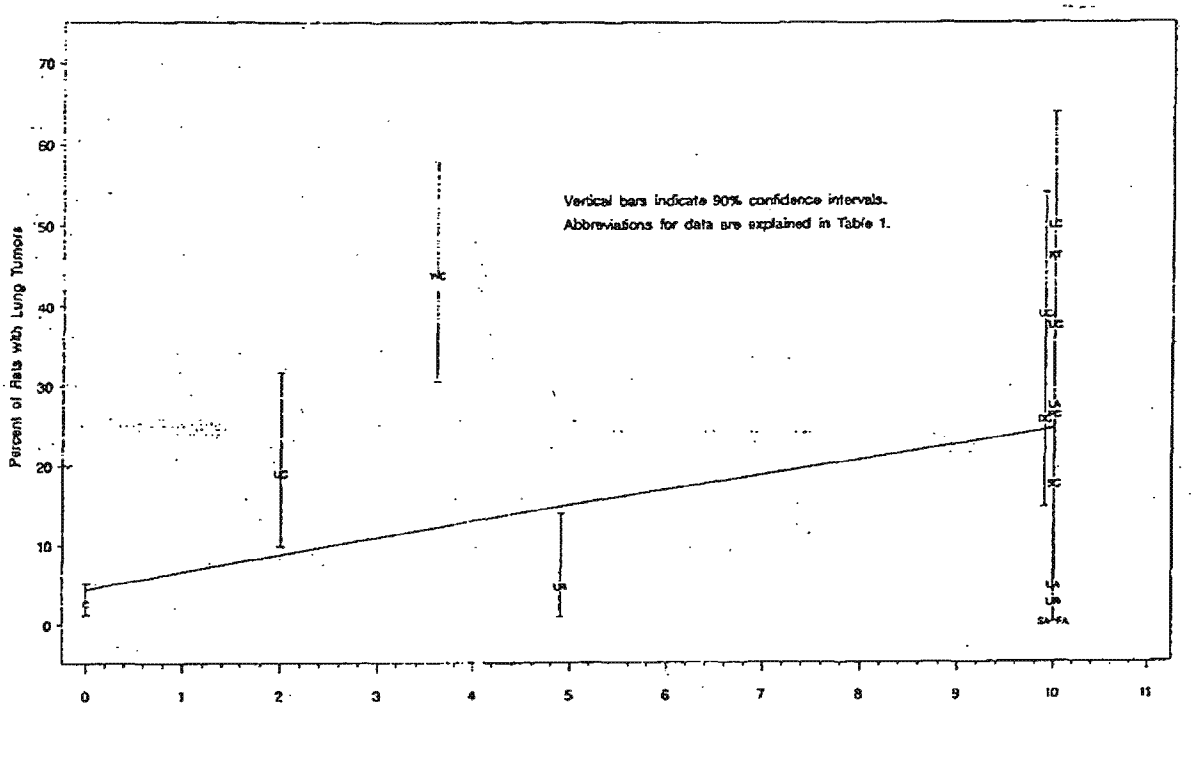

Fig. 1. Fit of model. Tumor incidence versus mass concentration from animal study.

to be zero so that the estimation results are the same as if these q_j's had not been included in the estimation procedure. Consequently these models may legitimately include more categories of asbestos structures than there are animal exposure groups.

Evaluation of Mesothelioma Incidence

Although there were too few mesotheliomas observed in the animal inhalation studies to perform an extensive analysis similar to that conducted for lung tumors, a test was conducted of whether the risk of mesothelioma was proportional to the risk development of lung tumors. If this test cannot be rejected, it suggests that any fiber size distribution that describes the lung tumor responses also describes the mesothelioma responses. The specific test conducted was a likelihood ratio test of whether the probability of mesothelioma could be expressed as

$$P_{meso} = cP_{ll}$$

where P_{meso} is the probability of developing mesothelioma following exposure; P_{ll} is the probability of developing lung tumors following exposure; and c is the constant of porpotionality between the probability of developing a mesothelioma and the probability of developing a lung tumor.

This test was applied to the total data set and to the chrysotile and amphibole studies separately.

RESULTS

Univariate Measures of Exposure

Figure 1 is a plot of the percentage of animals with lung tumors versus the mass concentrations (mg/m³) of total dust reported in the original Davis et al. studies. The curve in the figure represents the maximum likelihood fit of the dose-response model represented by Equation 4, where SM is the measured dust mass for each experiment reported in Table 1.

It is clear from Figure 1 that mass concentration of total dust does not provide a consistent dose-response

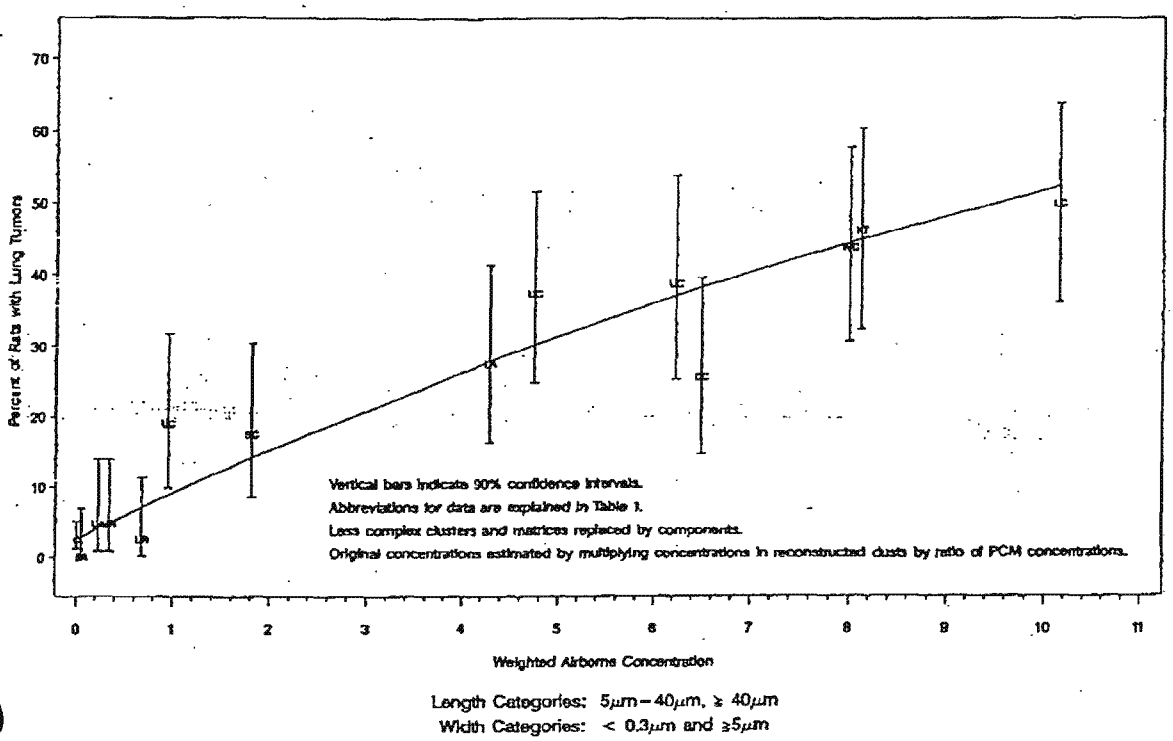

Fig. 2. Fit of model. Tumor incidence versus PCM concentration from animal study.

for these studies. Several of the Davis et al. studies employed a target mass concentration of 10 mg/m³ (Table 1) and results of these studies appear grouped together on the right side of the figure. Despite having been exposed to similar dust mass concentrations, responses in these animal groups are quite variable, ranging from 0 pct (0/42 animals) for short amosite to 50 pct (20/40 animals) for long chrysotile. Moreover, even though the experiment involving wet dispersed chrysotile involved exposure to a total dust mass concentration of only 3.5 mg/m³, the tumor response was 44 pct (18/41), which is considerably greater than that of several of the experiments employing a total mass concentration of 10 mg/m³.

Figure 2 is similar to Figure 1, except that the concentration of fibers measured by PCM (f/cc) in the original study replaces mass concentration as the measure of exposure. This figure likewise exhibits no consistent dose-response pattern. Thus, neither of the two measures of exposure reported in the original Davis et al. studies (total dust concentration and PCM fiber concentration) relate to lung tumor risk in a consistent manner.

Table 2 is a summary of the tests of goodness-of-fit for the exposure-response models presented in Figures 1 and 2 and similar models based on other univariate measures of exposure that are derived from TEM measurements of the re-generated dusts. For each univariate measure of exposure, the table contains the correlation coefficient (R^2) for the relationship between the airborne asbestos concentration (defined by the univariate measure) and the negative logarithm of the probability of remaining tumor-free [$-Ln(1-P)$]. The table also contains the deviance of the maximum likelihood fit of the univariate dose-response model (defined using Equation 4) and the p-value for the goodness-of-fit test associated with that deviance. Large deviances and, correspondingly, small p-values (i.e., $p \leq 0.05$) indicate a poor description of the lung tumor response by a particular univariate measure of exposure.

Both total dust mass and PCM concentrations give very large deviances and corresponding, highly significant lack of fit, 138.0 ($p \leq 0.0001$) and 56.1 ($p \leq 0.0001$), respectively (Table 2), which is consistent with the visual impressions from Figures 1 and 2. Likewise, the concentrations of total asbestos structures measured by TEM, of TEM structures longer than 5 μm, and of TEM structures longer than 20 μm all give poor fits to the data, although the deviance statistic decreases as the

Table II. Summary of Fits of Univariate Concentrations to Lung Tumor Data[a]

Dose measure	R^2	Deviance	*df*	*p*-value[a]
Total dust mass concentration	0.05	116.0	12	<0.0001
PCM structure concentration	0.50	56.1	12	<0.0001
Total TEM structure concentration[b]	0.32	112.1	12	<0.0001
Concentration of structure longer than 5 μm[b]	0.39	87.7	12	<0.0001
Concentration of structure longer than 10 μm[b]	0.50	51.4	12	<0.0001
Concentration of structure longer than 20 μm[b]	0.72	31.4	12	0.0017
Concentration of structure longer than 30 μm[b]	0.71	41.7	12	<0.0001
Concentration of structure longer than 20 μm and thinner than 0.4 μm[b]	0.60	37.41	12	0.0002
Concentration of structure longer than 20 μm and thinner than 0.2 μm[b]	0.29	92.9	12	<0.0001
Concentration of structure longer than 20 μm and thicker than 0.4 μm[b]	0.71	38.0	12	0.0002
Total structure surface area per air volume[c]	0.65	38.4	12	0.0001
Total structure volume per air volume[c]	0.54	50.2	12	<0.0001
Sum of aspect ratios per air volume[b]	0.32	108.8	12	<0.0001
Sum of (aspect ratio)$^{1.8}$ per air volume[b]	0.35	100.3	12	<0.0001
Stanton Index[b,d]	0.38	79.85	12	<0.0001

[a] P-values ≤0.05 indicate a significant lack of fit of model to lung tumor data, based on chi-square distribution for the defiance with 12 degrees of freedom (14 data sets and two parameters).
[b] Concentrations derived counting components of less complex structures as individual structures and ignoring the parent structure.
[c] Concentrations derived counting only primary structures.
[d] The index proposed by Stanton *et al.*[23] is the concentration of all fibers ≥ 8 μm in length and < 0.25 μm in width.

structures are restricted to increasing lengths in this series, which indicates an improving fit. However, restricting the analysis to even longer structures (≥ 30 μm), restricting the widths of structures longer than 20 μm to thinner structures (< 0.4 μm or < 0.2 μm) or to thicker structures (≥ 0.4 μm) all make the fit worse.

Several other measures evaluated in Table 2 are similar to exposure measures found by other investigators to be significantly correlated with tumor incidence: structures longer than 8 μm and thinner than 0.25 μm,[24] total surface area of the asbestos structures per unit volume of air (implied by Lippman,[41] assuming a relationship between tumor induction and fibrosis as described by Davis and Cowie[42]); total volume of asbestos per unit volume of air (which is proportional to the total mass concentration of asbestos[43]), the concentration of aspect ratios (sum of aspect ratios of structures per unit volume of air[29]); and the concentration of aspect ratios raised to the 1.8 power.[30]

All measures reported in Table 2 are significantly correlated ($p \leq 0.05$, based on the slope of the regression line) with lung tumor incidence. Nevertheless, all of these measures provide a poor fit to the lung tumor data ($p \leq 0.0017$, based on the deviance statistic) despite a significant correlation coefficient.

The results in Table 2 suggest that the tumorigenicity of the asbestos dusts studied by Davis et al. are more closely related to the concentration of longer structures than to the concentration of shorter structures. As previously suggested by Wylie et al.,[31] however, the fact that none of the exposure measures listed in Table 2 provide an adequate description of the database suggests that the features of asbestos that relate to risk are too complex to be represented by a single univariate exposure measure and that multivariate measures may be required to adequately describe lung tumor response to asbestos.

Multivariate Measures of Exposure

To gain an understanding of the combinations of structure categories that relate best to potency, more than 100 statistical analyses were conducted in which relative potencies were estimated for various combinations of length and width categories. The results of these exploratory analyses are summarized by an analysis that incorporates a matrix of five length categories (< 5 μm, 5–10 μm, 10–20 μm, 20–40 μm, and ≥ 40 μm in length) in combination with five categories of width (< 0.15 μm, 0.15–0.3 μm, 0.3–1.0 μm, 1.0–5.0 μm, and ≥ 5.0 μm in width), for a total of 25 categories of structures that potentially contribute independently to potency. In this analysis, the relationship between exposure and response was modeled using Equation 1 with WC consisting of a 25-term function that is the sum of the product of each size category multiplied by a relative potency for that size category (Equation 2). Table 3 indicates the maximum likelihood estimates of the relative

Table III. Relative Potencies for Inducing Lung Cancer[a]

	Width (μm)	Length (μm) < 5	5–10	10–20	20–40	> 40	Total
Analysis based on primary structures	< 0.15		0.0055	0.42	X	X	0.42
	0.15–0.3			0.040			0.040
	0.3–1.0						0
	1.0–5.0						0
	> 5.0	X		0.043	0.074	0.42	0.54
	Total	0	0.0055	0.50	0.074	0.42	1.0
	Deviance = 13.33 (7 *df*)						
	$p = 0.06$						
Less complex clusters and matrices replaced by components	< 0.15			0.033	0.10	X	0.13
	0.15–0.3		0.0018			0.72	0.72
	0.3–1.0						0
	1.0–5.0						0
	> 5.0	X			0.02	0.13	0.15
	Total	0	0.0018	0.033	0.12	0.85	1.0
	Deviance = 12.03 (7 *df*)						
	$p = 0.10$						

[a] Entries represent an estimate of the relative potency assigned to structures in that size category by the model defined by Equation (1). An "X" indicates a category that contains no structures. A blank indicates zero potency estimated for that category. *P*-value is for fit of model to lung tumor data in Table I, based on chi-square distribution for the deviance (small *p*-values indicate poor fits).

tencies (i.e., the q_j's from the model) of the structures each of the 25 size categories.

Table 3A presents results in which only primary uctures are included, whereas Table 3B presents re-lts in which parent clusters and matrices (for which mponent structures were characterized) are replaced their components. The statistical analysis in which mplex structures are resolved into components (Table 3) provides the best fit to the data and the resulting odel provides an overall adequate description of the ta based on goodness-of-fit (deviance = 12.03 [7 df], = 0.10). The fit is also marginally acceptable from the alysis (Table 3A) that includes only primary structures eviance = 13.33 [7 df], p = 0.06). These two analyses hibit several common features. Both of the analyses ribute zero potency to structures shorter than 5 μm. sitive potencies are confined to structures that are ei-r thin (< 0.3 μm) or very thick (≥ 5 μm). For both n and thick structures, potency tends to increase with creasing length, although the observed relationships : not entirely monotone.

Resolution of complex structures into component ers and bundles significantly increases the precision th which fibers and bundles can be categorized, since ighly 50 pct of the fibers and bundles characterized he re-generated dusts are components of complex ures. Consequently, from this point on, only analyses that resolve clusters and matrices into components are considered.

Although the statistical analysis reported in Table 3B adequately describes the data, the relative potencies assigned to the two narrowest categories of structures seems somewhat unrealistic; one expects dose-response relationships to vary smoothly with size. Positive potencies are assigned to structures thinner than 0.15 μm in combination with one long and one short length category (5–10 μm and ≥ 40 μm) and to structures between 0.15 and 0.3 μm in width in combination with two intermediate length categories (10–20 μm and 20–40 μm). This suggests that the potencies of structures in these two width categories cannot be distinguished using this database.

To test this hypothesis, these two categories were combined into a single category (width < 0.3 μm). The results of this analysis are presented in Table 4A. Combining these width categories only slightly increases the deviance (from 12.03 to 12.15), so that the hypothesis that structures in the two width categories are equally potent cannot be rejected. Moreover, the fit of the model actually improves somewhat (the p-value increases from 0.10 to 0.14), due to a reduction in the number of degrees of freedom.

Because the pattern of potencies observed among the length categories of the model presented in Table 4A

Table IV. Additional Analyses Performed to Obtain an "Optimum Exposure Index"*

	Width (μm)	Length (μm) < 5	5–10	10–20	20–40	> 40	Total
A: Intermediate analysis	< 0.3		0.0012	0.0054		0.84	0.847
	0.3–1.0						0
	1.0–5.0						0
	> 5.0	X			0.012	0.14	0.152
	Total	0	0.0012	0.0054	0.012	0.98	1.0
	Deviance = 12.15 (8*df*)						
	$p = 0.14$						
B: Optimum exposure index	< 0.30		0.0017			0.853	0.855
	> 5.0					0.145	0.145
	Total		0.0017			0.998	1.0
	Deviance = 12.66 (10 *df*)						
	$p = 0.24$						

* Entries represent an estimate of the relative potency assigned to structures in that size category by the model defined by Equation (1). An "X" indicates a category that contains no structures. A blank indicates zero potency estimated for that category. *P*-value is for fit of model to lung tumor data in Table I, based on chi-squared distribution for the deviance. (Small *p*-values indicate poor fits).

also appear somewhat unrealistic, this model was simplified by reducing the number of length categories in the same manner that the number of width categories was reduced for the model described above. Therefore, structures between 5 μm and 40 μm in length were combined into a single length category. Also, structures shorter than 5 μm were removed from the analysis because, even with the reduced number of length categories, the short structures were assigned zero potency. Structures between 0.3 and 5.0 μm in width were also removed because these too were assigned zero potency in the reduced model.

The model resulting from the maximum likelihood fit of the remaining size categories (referred to as the "optimum exposure index") is shown in Table 4B. The deviance of 12.66 obtained from this analysis is only slightly larger than that of the full model (12.03) and the goodness-of-fit p-value from the reduced model is 0.24 (10 df), which indicates a better statistical fit than was obtained using the original model (Table 3B) or the intermediate model (Table 4A).

The "optimum exposure index" assigns a relative potency of:

- 0.0017 for structures < 0.3 μm in width and between 5 and 40 μm in length;
- 0.853 for structures < 0.3 μm in width and ≥ 40 μm in length; and
- 0.145 for structures ≥ 5.0 μm in width and ≥ 40 μm in length.

All other structures are assigned a potency of zero in the optimum exposure index. Interestingly, whereas the latter size category is composed completely of complex structures, the two categories of thin structures are composed almost totally of fibers and bundles (including many that are components of complex structures).

The fit to the experimental data obtained by the "optimum exposure index" is presented in Figure 3. The x-axis of this plot is exposure expressed as the weighted airborne concentration formed by the sum of the relative potencies from this analysis times the concentrations of structures in the corresponding categories (WC in Equation 2). Unlike Figures 1 and 2, this graph indicates a consistent dose-response relationship.

Table 5 contains 90 pct confidence intervals for the three structure categories that are assigned positive potency by the optimum exposure index. The fact that none of these three confidence intervals contains zero potency implies that none of these three structure categories can be removed from the model without significantly degrading the fit (i.e. the hypothesis that one of these categories has zero potency can be rejected). Thus, to obtain adequate fits to the lung tumor incidence data within the framework of this analysis, it is necessary to assign positive potencies to all three of the size categories of structures that contribute to the optimum exposure index.

Table 5 also contains 90 pct confidence intervals for two categories of structures assigned zero potency in the optimum exposure index: structures < 5 μm in length and structures 5–40 μm in length and ≥ 5 μm in thickness. The upper 95 pct confidence bound for the relative potency of structures shorter than 5 μm is estimated as 0.00008. This upper bound is 0.00008/0.0017

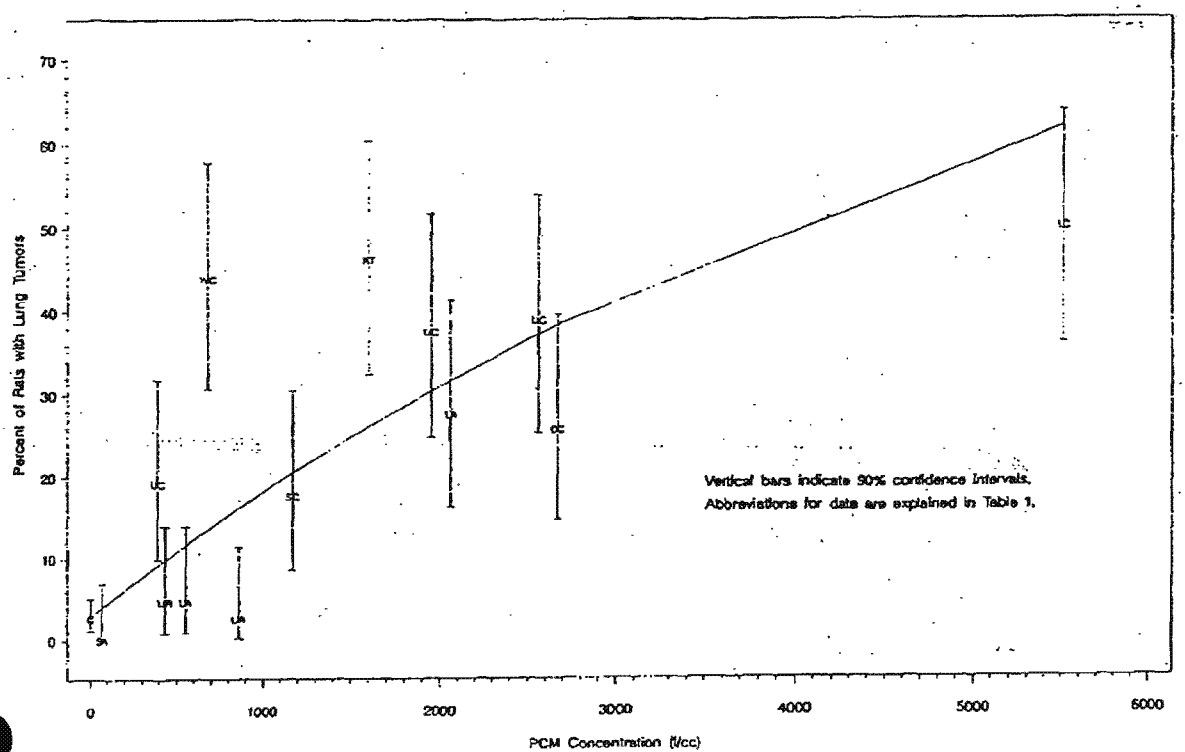

Fig. 3. Fit of model. Tumor incidence versus structure concentration by TEM.

Table V. Relative Potency Estimates Derived from the "Optimum Exposure Index" with 90% Confidence Intervals

Category (units in μm)	Relative potency estimate	90% confidence interval
length < 5	0	[0, 0.00008]*
5 ≤ length < 40 width ≤ 0.3	0.0017	[0.0010, 0.0032]
5 ≤ length < 40 width ≥ 5.0	0	[0, 0.030]*
length ≥ 40 width < 0.3	0.85	[0.67, 0.95]
length ≥ 40 width ≥ 5.0	0.15	[0.04, 0.32]

* The size category is assigned zero potency in the model derived from the maximum likelihood fit and therefore does not contribute to the "optimum exposure index."

= 1/20 as large as the estimated relative potency of structures between 5 and 40 μm in length and thinner than 0.3 μm, and only 0.00008/0.85 = 1/10,000 as large as the estimated relative potency of structures longer than 40 μm and thinner than 0.3 μm.

Results of various additional hypothesis tests are presented in Table 6. All of the analyses presented indicate a zero potency for all categories of structures shorter than 5 μm. Since this is the outcome most favorable to the hypothesis that such structures are non-potent, p = 1.0 is the p-value associated with a test of this hypothesis. Although some analyses reported herein assign a positive potency to structures 5–10 μm in length, the hypothesis that structures shorter than 10 microns in length are non-potent cannot be rejected either (p = 0.09).

Results of hypothesis tests for a difference between the potency of chrysotile and amphibole, conducted within the framework of the optimum exposure index, are also presented in Table 6. This test was performed by estimating different absolute potencies (i.e., different values for β; in the model) for chrysotile and amphibole, but assuming that the relative potencies of structures in different size categories (i.e., the q_j's) are the same for chrysotile and amphibole (Equation 3). The resulting p-value for this test is 0.72 (non-significant), indicating no detectable difference between the potency of chrysotile and amphibole. It is also *not* possible to reject the com-

pound hypothesis that chrysotile and amphibole have the same relative potencies *and* that the relative contributions to potency from different size fractions are the same for chrysotile and amphibole.

The optimum exposure index assigns positive potency to thin (< 0.3 μm) and very thick (> 5 μm) structures but not to structures of intermediate thickness. Although a potency for very thick structures could be due to thin structures imbedded within complex structures (see discussion), this result could also be an artifact caused by limitations in the data base and the specific cutpoints used to create the optimum exposure index. Additional analyses taken to further explore this issue identified a slightly different index that also provides an adequate fit to the data (p = 0.09) and which does not result in a positive potency for very thick structures. This index assigns a relative potency of:

- 0.0024 for structures < 0.4 μm in width and between 5 and 40 μm in length; and
- 0.9976 for structures < 0.4 μm in width and ≥ 40 μm in length.

Table VI. Hypothesis Test Results for Lung Tumor Incidence

	Decrease in deviance	*P*-value of Hypothesis test[a]	
Structures shorter than 5 μm are non-potent	0	1	(NS)[b]
Structures shorter than 10 μm are non-potent[c]	1.76	0.09	(NS)
Structures shorter than 40 μm are non-potent[d]	74.6	<0.0001	(S)[e]
Structures longer than 40 μm are non-potent[d]	73.1	<0.0001	(S)
Structures thicker than 5 μm are non-potent[d]	10.0	0.007	(S)
Structures thinner than 0.3 μm are non-potent[d]	54.4	<0.0001	(S)
Amphibole and chrysotile structures are equally potent[d]	0.12	0.72	(NS)
Fibers and bundles are equally potent[d]	0.78	0.68	(NS)

[a] A P-value less than 0.05 indicates that the hypothesis can be rejected.
[b] NS - not significant (hypothesis cannot be rejected).
[c] Based on analysis of data in Table 5A.
[d] Based on analysis of data in Table 5B.
[e] S - significant (hypothesis can be rejected).
[f] Due to a limitation in the computer program used to perform these calculations, the value of the background parameter, α, was fixed at the value that provides a perfect fit to the control data.

Statistical Analyses of Mesothelioma Data

Results in Table 7 indicate that the hypothesis that mesothelioma incidence is proportional to lung tumor incidence for all sample types combined can be rejected. However, the hypotheses that mesothelioma incidence is proportional to lung tumor incidence either for chrysotile sample types or amphibole sample types (considered separately) cannot be rejected.

The best indication (i.e., maximum likelihood) is that the probability of a chrysotile (amphibole) exposure inducing mesothelioma is 0.058 (0.20) times the probability that the same exposure induces lung tumors. These two values are significantly different (p = 0.032). Since the analyses of the lung tumor data indicate that there is no difference between chrysotile and amphibole in their ability to induce lung tumors, these results suggest that amphibole is 0.20/0.058 = 3.4 times more potent than chrysotile for causing mesothelioma in rats (assuming that the relative potencies of structures in different size categories are approximately the same for mesothelioma and lung tumors.

DISCUSSION

Results from this study indicate that the induction of lung tumors in rats following inhalation of asbestos is a function of the size and shape of asbestos structures within the inhaled dusts. Structures contributing to lung tumor risk appear to be long (≥ 5 μm) thin (< 0.3 or 0.4 μm) fibers and bundles, with a possible contribution by long and very thick (≥ 5 μm) complex clusters and matrices. Potency appears to increase with increasing length, with structures longer than 40 μm being about 500 times more potent than structures between 5 and 40 μm in length. Fibers and bundles of similar dimensions appear to contribute equally to potency.

For all types of asbestos structures, results of this study suggest that a minimum length (between 5 and 10 μm) exists such that the best estimate of the potency of structures shorter than this minimum is zero. This analysis also indicates that, as a worst case, a 95% upper limit to the potency of individual structures shorter 5 μm is no more than about 1/20 of the potency estimated for individual fibers or bundles between 5 and 40 μm in length and no more than about 1/10,000 of that estimated for individual fibers or bundles ≥40 μm in length and <0.3 μm in width. In contrast, the evidence suggesting a range of widths within which structures can be considered non-potent is less compelling.

Table VII. Hypothesis Test Results for Comparing Mesothelioma and Lung Tumor Incidence

Hypothesis tested	Increase in deviance	*P*-value of hypothesis test[a]
The relative probability of inducing mesotheliomas and lung tumors are the same for all dusts tested. ($P_{meso} = cP_L$)[b]	20.9	0.028
The relative probability of inducing mesotheliomas and lung tumors are the same for all chrysotile dusts tested. ($P_{meso} = c_1P_L$)[c]	9.97	0.20
The relative probability of inducing mesotheliomas and lung tumors are the same for all amphibole dusts tested. ($P_{meso} = c_2P_L$)[d]	6.30	0.28
The proportionality constant relating mesothelioma incidence to lung tumors incidence is the same for chrysotile and the amphiboles ($c_1 = c_2$)	4.62	0.032

[a] A *P*-value less than 0.05 indicates that *P* is significant and the hypothesis can be rejected.
[b] The best estimate for the constant of proportionality between mesothelioma and lung tumor incidence is $c = 0.094$ when all dusts are considered.
[c] The best estimate for the constant of proportionality betwen mesothelioma and lung tumor incidence is $c_1 = 0.058$ when chrysotile dusts are considered separately.
[d] The best estimate for the constant of proportionality between mesothelioma and lung tumor incidence is $c_2 = 0.20$ when amphibole dusts are considered separately.

For mesothelioma, it appears that mineralogy is an important determinant of the relative potency of inhaled dusts, with chrysotile being less potent toward the induction of mesotheliomas than the amphiboles in comparison to their relative potency for inducing lung tumors.

Despite the special emphasis placed on the characterization of long structures, the data base employed in this study contains only a limited number of very long structures (e.g., ≥40 μm in length). This contributes uncertainty to the specific quantitative estimates of relative potency for long structures, the most potent structures identified. Our statistical analysis does not address this type of uncertainty; fiber concentrations were assumed to be known with certainty. Additional uncertainties in the exposure estimates result from the reliance on regenerated dusts in this study rather than the actual dusts to which the experimental animals were exposed. This problem was mitigated by having the dusts regenerated by the same personnel using the same stock material, equipment, and procedures that were employed in the original studies.

Despite the above considerations, we know of no other set of experimental data that is more suitable for quantitative determination of relative potencies of asbestos structures of different types and dimensions that are apt to be relevant to conditions of human exposure. Our study involves inhalation, which is more relevant to human exposures than injection or implantation studies. Our data base contains data on a variety of different types of asbestos including crocidolite, tremolite, chrysotile, and amosite. It includes four different samples of chrysotile and three different samples of amosite, which were chosen to represent a range of asbestos structure size dimensions. It also involves a more detailed characterization of long structures and complex structures than those available from other experimental settings.

The only other studies in which the relationship between structure size and shape and tumor response has been examined formally (using some type of statistical analysis) are the studies by Stanton et al.[23,24] and other statistical studies employing the database reported by Stanton et al.[29,30] or employing a re-analysis of the samples studied by Stanton and coworkers.[31] However, these studies all incorporate a statistical procedure that differs radically from that employed in the present study. While the earlier studies only identify exposure measures that are significantly correlated with tumor incidence, the present study identifies an exposure measure that satisfactorily describes the tumor incidence (i.e., provides an acceptable fit to all of the data).[6] In fact, it

[6] The methodology utilized in this study avoids several methodological problems associated with the analysis by Stanton et al. and the others who re-evaluated their data and conclusions. Stanton et al. computed a correlation between the logarithm of the concentration of fibers in specific dimensional ranges and the logit of the probability of a tumor. A number of exposure categories for individual fiber types investigated by Stanton et al. contained no fibers, which implies that the logarithm of the fiber concentration for these categories is undefined. Stanton et al. assigned a zero in place of the logarithm of concentration in these cases. However, this decision is entirely arbitrary and the value selected could have had a large impact upon the correlation coefficient. Similarly, no tumors were detected in several experimental groups investigated by Stanton et al. and the logit is undefined whenever no tumors occur. Although it is not clear how Stanton et al. handled this problem, it seems likely that such groups were omitted from their analysis. Note that, because of these problems, the correlation coefficients presented in Table 2 (which are calculated based on a linear relationship that is not undefined at zero) may *not* be directly comparable to those calculated by Stanton et al.

is apparent from Text Figure 2 of Stanton et al.[24] that the exposure measure they identify as being most highly correlated with tumor incidence (fibers longer than 8 μm and thinner than 0.25 μm) does not provide an acceptable fit to the observed tumor incidence. Similarly, although all of the univariate measures considered in the present study (Table 2) are highly correlated with tumor incidence, none of them adequately describe lung tumor incidence.

In contrast, when asbestos exposure is expressed as the weighted sum of the concentrations of structures in the three size categories of structures defined in this study by the optimum exposure index, this exposure index provides a statistically adequate fit to the lung tumor response data reported in the studies by Davis et al. (Table 1). Consequently, the hypothesis that the model determined by the optimum exposure index completely characterizes the potency of asbestos structures in the induction of lung tumors in AF/HAN rats cannot be rejected. This implies that this model can potentially provide adequate descriptions of risk in a broader range of exposure settings.

Stanton et al.[24] found that fibers longer than 8 μm appear to correlate best with mesothelioma incidence, which parallels the findings in this study that structures longer than some minimum length (between 5 and 10 μm) tend to contribute to the induction of lung tumors following inhalation and that potency tends to increase with increasing length. However, our analysis indicates that the potency of structures increases with length up to lengths of at least 40 μm, whereas Stanton et al. did not explicitly consider the contribution to potency by such long structures.

The maximum thickness for potent fibers and bundles found in this study (< 0.3 or 0.4 μm) is comparable to the maximum thickness reported by Stanton et al.[24] of 0.25 μm. Stanton et al. did not report information on complex structures in their data base and, indeed, the meaning of complex structures in a gel suspension (which they used for implantation) is not clear. Consequently, their study provided no information on the effects of thick clusters. Complex asbestos structures do occur as isolated species in the air, however, and results in this study indicate that clusters longer than 40 μm and thicker than 5 μm may contribute to the potency of an asbestos dust.

That long, thick clusters (structure for structure) may contribute about one-sixth as much to total potency as long, thin fibers or bundles (Table 5B) suggests a mechanism in which some of these may break down and liberate long fibers or bundles that may then contribute to the induction of tumors. The structures longer than 40 μm and thicker than 5 μm that are evaluated in this study are open structures with settling velocities that are likely comparable to their component fibers or bundles. Thus, it is likely that they are respirable and can penetrate the deep lung. Once in the deep lung, however, when such structures impact a wall, some may liberate component fibers or bundles and the longest and thinnest of those may then contribute to the induction of tumors.

Although neither Stanton et al.[23,24] nor Bertrand and Pezerat[29] concluded that mesothelioma induction following injection or implantation is a strong function of fiber mineralogy, such a conclusion was reached by Bonneau et al.[30] In our study, there is no evidence that mineralogy is a determinant of potency toward the induction of lung tumors. However, assuming the size range that induces lung tumors and mesothelioma are similar, results in this study suggest that for inhaled dusts that exhibit comparable potency toward lung tumor induction, amphibole dusts are approximately three times as likely to induce mesothelioma as chrysotile dusts.

Implications for Human Exposure

For human exposures, potency estimates obtained from different epidemiological studies, which are based upon PCM measurements, have been found to differ by large factors.[1] This study likewise demonstrates that PCM measurements do not provide a consistent dose response in the animal inhalation studies either. However, more complex exposure measures based upon TEM measurements are shown to provide a consistent dose-response relationship for the animal data. This suggests that the observed lack of a consistent dose response across epidemiological studies is due at least partially to the fact that the features of asbestos important to determining potency are not adequately represented by PCM measurements.

Regarding mineralogy, human epidemiology studies (taken as a whole) suggest that mineralogy is important at least for determining potency toward the induction of mesothelioma.[1] Our results likewise indicate that amphibole dusts are more likely (by a factor of about three) to induce mesothelioma than chrysotile dusts whenever their potential to induce lung tumors are comparable.

The importance of mineralogy in determining the relative potency of a dust toward the induction of lung tumors in human exposure is less clear.[1] Results from this study suggest that, when the relative size distribution of structures in a dust is taken into account, the miner-

alogy of a structure does not contribute to the determination of potency toward the induction of lung tumors. However, this finding may not be applicable to humans because chrysotile degrades more rapidly than amphibole *in vivo*. Since humans live much longer than the animal species typically used in experiments, the relative persistence of chrysotile and amphibole *in vivo*[1] may have a much larger impact on the induction of lung tumors in humans while remaining unimportant in animals.

Implications for Asbestos Measurement

Results from this study indicate strongly that methods for the measurement of asbestos should be modified to include better characterization of longer structures and that such characterization should be performed using TEM (as opposed to PCM), due to the need to include thin structures (and the need to distinguish asbestos structures from non-asbestos structures). Better characterization of longer structures can be achieved, just as in our reanalysis of the data from the animal experiments, by examination of grid specimens at lower magnifications in which only structures exceeding some minimum length are recorded. At a minimum, we recommend that separate examinations be made for structures ≥ 5 μm in length. However, because of the indication in this study that very long structures (≥ 40 μm in length) are highly potent relative to shorter structures, we also recommend that a separate examination of still longer structures (e.g., structures ≥ 20 μm in length) be included in the routine analysis of asbestos. Similarly, to obtain exposure measures that relate more closely to risk without unduly increasing the cost of the analysis, characterization of structures shorter than 5 μm can be deemphasized.

ACKNOWLEDGMENTS

We wish to thank Kent Kitchingman and Steven Bayard for their advice and support. We also acknowledge the National Asbestos Task Force of the U.S. Environmental Protection Agency, chaired by Hans Crump, for funding this work. Recognition is extended to Mike Whittington, who generated the dust clouds and collected the samples; Greg Lewis and Alice Liebert, who performed the many hours of TEM analysis required; Jane Chatfield who completed the quality assurance work to confirm data quality; Tammie Lambert and Shipei Weng, who performed the data manipulation and regression analyses; and Robyn York and Lynn Williams for typing the revisions to this manuscript. The work could not have been completed without each of their contributions. Finally, we wish to remember Richard Howe who developed the software we used to complete the regression analyses reported in this study.

REFERENCES

1. HEI-AR (Health Effects Institute-Asbestos Research), "*Asbestos in Public and Commercial Buildings: A Literature Review and Synthesis of Current Knowledge*" (HEI-AR, 141 Portland St., Suite 7100, Cambridge, Massachusetts, 1991).
2. USEPA (United States Environmental Protection Agency), *Airborne Asbestos Health Assessment Update* (Office of Health Effects Assessment, Washington, D.C., Report 600/8-84-003F, 1986).
3. W.H. Walton, "*The Nature, Hazards and Assessment of Occupational Exposure to Airborne Dust: A Review.*" Annals of Occupational Hygiene 26, 115–247.
4. R.E. Bolton, J.M.G. Davis, K. Donaldson, and A. Wright, "Variation in the Carcinogenicity of Mineral Fibres," *Annals of Occupational Hygiene*, 26, 569-582 (1982).
5. R.E. Bolton, J.M.G. Davis, B.G. Miller, K. Donaldson, and A. Wright, "The Effect of Dose of Asbestos on Mesothelioma Production in the Laboratory Rat," *Proceedings of the VIth International Pneumoconiosis Conference*, 2, 1028-1035 (1984).
6. R.E. Bolton, J. Addison, J.M.G. Davis, K. Donaldson, A.D. Jones, B.G. Miller, and A. Wright, "Effects of the Inhalation of Dusts from Calcium Silicate Insulation Materials in Laboratory Rats," *Environmental Research*, 39, 26-43 (1986).
7. J.M.G. Davis, S.T. Beckett, R.E. Bolton, P. Collings, and A.P. Middleton, "Mass and Number of Fibres in the Pathogenesis of Asbestos-Related Lung Disease in Rats," *British Journal of Cancer*, 37, 673-688 (1978).
8. J.M.G. Davis, S.T. Beckett, R.E. Bolton, and K. Donaldson, "A Comparison of the Pathological Effects in Rats of the UICC Reference Samples of Amosite and Chrysotile with Those of Amosite and Chrysotile Collected from the Factory Environment" (J.C. Wagner, ed., *Biological Effects of Mineral Fibres*, IARC Scientific Publications, 288-292, 1980).
9. J.M.G. Davis, J. Addison, R.E. Bolton, K. Donaldson, A.D. Jones, and R.G. Miller, "Inhalation Studies on the Effects of Tremolite and Brucite Dust in Rats," *Carcinogenesis*, 6, 667-674 (1985).
10. J.M.G. Davis, J. Addison, R.E. Bolton, K. Donaldson, A.D. Jones, and T. Smith, "The Pathogenicity of Long Versus Short Fibre Samples of Amosite Asbestos Administered to Rats by Inhalation and Intraperitoneal Injection," *British Journal of Experimental Pathology*, 67, 415-430 (1986).
11. J.M.G. Davis, J. Addison, R.E. Bolton, K. Donaldson, and A.D. Jones, "Inhalation and Injection Studies in Rats Using Dust Samples from Chrysotile Asbestos Prepared by a Wet Dispersion Process," *British Journal of Pathology*, 67, 113-129 (1986).
12. J.M.G. Davis, R.E. Bolton, A.N. Douglas, A.D. Jones, and T. Smith, "Effects of Electrostatic Charge on the Pathogenicity of Chrysotile Asbestos," *British Journal of Industrial Medicine*, 45, 292-309 (1988).
13. J.M.G. Davis, and A.D. Jones, "Comparisons of the Pathogenicity of Long and Short Fibres of Chrysotile Asbestos in Rats," *British Journal of Exposure Pathology*, 69, 171-738 (1988).
14. E.J. King, J.W. Clegg, V.M. Rae, "The Effects of Asbestos, and of Asbestos and Aluminum, on the Lungs of Rabbits," *Thorax*, 1, 188-197 (1946).

15. H. Muhle, B. Bellmann, S. Takenata, and U. Ziem, "Inhalation and Injection in Rats to Test the Carcinogenicity of MMMF," *Annals Occupational Hygiene*, 31, 755-764 (1987).
16. F. Pott, F. Huth, and K.H. Friedrichs, "Tumorigenic Effect of Fibrous Dust in Experimental Animals," *Environmental Health Perspectives*, 9, 313-315 (1974).
17. F. Pott, F. Huth, and K.H. Friedrichs, "Results of Animal Carcinogenesis Studies After Application of Fibrous Glass and Their Implications Regarding Human Exposure" (*Occupational Exposure to Fibrous Glass*, U.S. HEW Publication No. 76-151, pp. 183-191, 1976).
18. F. Pott, "Some Aspects on the Dosimetry of the Carcinogenic Potency of Asbestos and Other Fibrous Dusts," *Staub-Reinhalt*, 38. 486-490 (1978).
19. F. Pott and H. Muhle, "Animal Experiments with Mineral Fibres" Proceedings from a symposium, *Short and Thin Mineral Fibres: Identification, Exposure, and Health Effects*, National Board of Occ. Safety and Health, Solnic, Sweden pp. 133-161, 1982).
20. F. Pott, U. Ziem, and U. Mohr, "Lung Carcinomas and Mesotheliomas Following Intratracheal Instillation of Glass Fibres and Asbestos" (*Proceedings of the 6th Pneumoconiosis Conference*, pp. 747-756, 1983).
21. F. Pott, U. Ziem, R.J. Reiffer, F. Huth, H. Ernst, and U. Mohr, "Carcinogenicity Studies on Fibres, Metal Compounds, and Some Other Dusts in Rats," *Experimental Pathology*, 32, 129-152 (1987).
22. M. Stanton, and C. Wrench, "Mechanisms of Mesothelioma Induction with Asbestos and Fibrous Glass," *Journal of the National Cancer Institute*, 48, 797-821 (1972).
23. M. Stanton, M. Layard, A. Tegeris, E. Miller, M. May, and E. Kent, "Carcinogenicity of Fibrous Glass: Pleural Response in the Rat in Relation to Fiber Dimension," *Journal of the National Cancer Institute*, 58, 587-597 (1977).
24. M. Stanton, M. Layard, A. Tegeris, E. Miller, M. May, and E. Morgan, "Relation of Particle Dimension to Carcinogenicity in Amphibole Asbestos and Other Fibrous Minerals," *Journal of the National Cancer Institute*, 67, 965-975 (1981).
25. J.C. Wagner, G. Berry, and J.W. Skidmore, "Studies of the Carcinogenic Effects of Fiber Glass of Different Diameters Following Intrapleural Inoculation in Experimental Animals" (*NIOSH 76-151*, pp. 193-197, 1976).
26. J.C. Wagner, G. Berry, R.J. Hill, D. Munday, and J.W. Skidmore, "Animal Experiments with MMM(V)F-Effects of Inhalation and Intrapleural Inoculation in Rats. Biological Effects of Man-made Fibres" (*Proceedings of a WHO/IARC Conference*, Copenhagen, pp. 209-233, 1982).
27. M.M.F. Wagner, J.C. Wagner, R. Davies, and D.M. Griffith, "Silica-Induced Malignant Histiocytic Lymphoma: Incidence Linked with Strain of Rat and Type of Silica," *British Journal of Cancer*, 41, 908-917 (1980).
28. J.C. Wagner, J.W. Skidmore, R.J. Hill, and D.M. Griffith, "Erionite Exposure and Mesotheliomas in Rats," *British Journal of Cancer*, 51, 727-730 (1985).
29. R. Bertrand and H. Pezerat, "Fibrous Glass: Carcinogenicity and Dimensional Characteristics. *Biological Effects of Mineral Fibres*" (J.C. Wagner, ed., *IARC Scientific Publications*, 901-911, 1980).
30. L. Bonneau, C. Malard, and H. Pezerat, "Studies on Surface Properties of Asbestos," *Environmental Research* 41, 268-275 (1986).
31. A.G. Wylie, R.L. Virta, and J.M. Segretti, "Characterization of Mineral Population by Index Particle: Implications for the Stanton Hypothesis," *Environmental Research*, 43, 427-439 (1987).
32. K.P. Lee, C.E. Barras, R.S. Griffith, R.S. Waritz, and C.A. Lapin, "Comparative Pulmonary Responses to Inhaled Inorganic Fibers with Asbestos and Fiberglass," *Environmental Research*, 24, 167-191 (1981).
33. E. McConnell, J.C. Wagner, J.W. Skidmore, and J. Moore, "A Comparative Study of the Fibrogenic and Carcinogenic Effects of UICC Canadian Chrysotile B Asbestos and Glass Microfibre (JM 100)" (*Biological Effects of Man-made Fibres*, Proceedings of a WHO/IARC Conference, pp. 234-252, 1982).
34. D.M. Smith, L.W. Oritiz, R.F. Archuleta, and N.F. Johnson, "Long-Term Health Effects in Hamsters and Rats Exposed Chronically to Man-Made Vitreous Fibres," *Annals of Occupational Hygiene*, 34, 731-754 (1987).
35. J.W. Wagner, G. Berry, J.W. Skidmore, and V. Timbrell, "The Effects of the Inhalation of Asbestos in Rats," *British Journal of Cancer*, 29, 252-269 (1974).
36. J.C. Wagner, D.M. Griffiths, and D.E. Munday, "Experimental Studies with Palygorskite Dusts," *British Journal of Industrial Medicine*, 44, 749-763 (1987).
37. E.J. Chatfield, and D.W. Berman, "*Interim Superfund Method for the Determination of Asbestos in Ambient Environments, Part 1: Method*" (USEPA publication: 540/2-90/005a, May 1990).
38. D.W. Berman and E.J. Chatfield, "*Interim Superfund Method for the Determination of Asbestos in Ambient Environments, Part 2: Technical Background Document*" (USEPA publication: 540/2-90/005b, May, 1990).
39. D. Cox and D. Lindley, *Theoretical Statistics*. (Chapman and Hall, London, 1974).
40. National Research Council, *Health Effects of Exposure to Low Levels of Ionizing Radiation. BEIR V. Committee on the Biological Effects of Ionizing Radiations* (National Academy Press, Washington, D.C., 1990).
41. M. Lippman, "Review: Asbestos Exposure Indices," *Environmental Research*, 46, 86-106 (1988).
42. J.M.G. Davis, and H. Cowie, "The Relationship Between Fibrosis and Cancer in Experimental Animals Exposed to Asbestos and Other Fibers," *Environmental Health Perspectives*, 88, 305-309 (1990).
43. W.J. Nicholson, *Airborne Levels of Mineral Fibres in the Non-Occupational Environment* (Division of Environmental and Occupational Medicine, Mt. Sinai School of Medicine, City University of New York, 1988).